ELSEVIER

Journal of Neuroscience Methods 106 (2001) 101–110

JOURNAL OF NEUROSCIENCE METHODS

www.elsevier.com/locate/jneumeth

Optimal filtering of whole nerve signals

Sašo Jezernik [a,*], Warren M. Grill [b]

[a] *Swiss Federal Institute of Technology, Automatic Control Laboratory, Physikstrasse 3, ETH Zürich/ETL K 28, CH-8092 Zürich, Switzerland*
[b] *Case Western Reserve University, Dept. of Biomedical Engineering, Cleveland, OH 44106-4912, USA*

Received 6 September 2000; received in revised form 22 January 2001; accepted 26 January 2001

Abstract

Electroneurographic recordings suffer from low signal to noise (S/N) ratios. The S/N ratio can be improved by different signal processing methods including optimal filtering. A method to design two types of optimal filters (Wiener and Matched filters) was developed for use with neurographic signals, and the calculated filters were applied to nerve cuff recordings from the cat S1 spinal root that were recorded during the activation of cutaneous, bladder, and rectal mechanoreceptors. The S1 spinal root recordings were also filtered using various band-pass (BP) filters with different cut-off frequencies, since the frequency responses of the Wiener and Matched filters had a band-pass character. The mean increase in the S/N ratio across all recordings was 54, 89, and 85% for the selected best Wiener, Matched, and band-pass filters, respectively. There were no statistically significant differences between the performance of the selected filters when all three methods were compared. However, Matched filters yielded a greater increase in S/N ratio than Wiener filters when only two filtering techniques were compared. All three filtering methods have in most cases also improved the selectivity of the recordings for different sensory modalities. This might be important when recording nerve activity from a mixed nerve innervating multiple end-organs to increase the modality selectivity for the nerve fibers of interest. The mean Modality Selectivity Indices (MSI) over different receptor types and for the same selected filters as above were 1.12, 1.27, and 1.29, respectively, and indicate increases in modality selectivity (MSI > 1). Improving the S/N ratio and modality selectivity of neurographic recordings is an important development to increase the utility of neural signals for understanding neural function and for use as feedback or control signals in neural prosthetic devices. © 2001 Published by Elsevier Science B.V.

Keywords: Signal processing; Nerve cuff electrodes; Neural recording; Electrophysiology

1. Introduction

Electroneurographic recordings are widely used to study the neurophysiology of the central and peripheral nervous systems (Hoffer et al., 1990; Loeb and Peck, 1996), and to extract sensory and/or motor information from the nervous system for use as feedback or control signals in neural prosthetic devices (Popovic et al., 1993; Sinkjaer et al. 1999). Neurographic electrodes record electric potentials caused by ionic currents flowing from nerve fibers into the surrounding volume conductor (Stein and Pearson, 1971). Since the electric potential drops rapidly with the distance from the source (neuron) to the recording electrode (Struijk, 1997), the recorded signals are rather small in amplitude (range of μV). The signals are also contaminated by external noise sources, by the thermal noise originating from the electrode-tissue impedance, and by noise in the electronics. The result is relatively low signal to noise (S/N) ratios of neurographic recordings (Nikolic et al., 1994). For example, for neurograms recorded by intrafascicular electrodes the average S/N ratio was three (4.8 dB) (Goodall and Horch, 1992), and for neurograms recorded by nerve cuff electrodes average S/N ratio ranged from 1–2 (0–3 dB) (Upshaw and Sinkjaer, 1998), and can often be less than 1 (< 0 dB).

Whole nerve recording yields a measured signal that results from superposition of the electrical activity of different active single fibers present in the nerve. The nerve signal can be modeled as a temporal and spatial summation of traveling action potentials. The signal has a zero mean, a variance proportional to the number

* Corresponding author.
E-mail addresses: jezernik@aut.ee.ethz.ch (S. Jezernik), wmg@po.cwru.edu (W.M. Grill).

0165-0270/01/$ - see front matter © 2001 Published by Elsevier Science B.V.
PII: S0165-0270(01)00334-X

of simultaneously recorded action potentials, and a Gaussian probability density function (Jezernik and Sinkjaer, 1999). The frequency spectrum of the nerve signal depends on the electrode geometry and configuration, and on the shape of the recorded action potentials composing the signal. A nerve signal composed of action potentials having longer durations (traveling at a slower conduction velocity) will have a lower frequency spectrum than a nerve signal composed of action potentials having shorter durations (traveling at a faster conduction velocity). This fact actually allows frequency filtering techniques to increase the modality selectivity when recording from a mixed nerve in the case that different end-organs (modalities) are innervated by nerve fibers conducting with different conduction velocities. The frequency spectrum of a nerve signal usually ranges from a few hundred Hz to a few thousand Hz. This range overlaps with the frequency range of the noise signal (see also Fig. 4A where the spectrum of the noise N is estimated), which makes filtering of the noise component difficult.

The S/N ratio can be increased by optimizing the nerve-electrode interface, by applying different noise reduction techniques, or by advanced signal processing methods. In this report, a method to design optimal Wiener and Matched filters for neurographic recordings is introduced. Wiener filters attenuate the noise contaminating the true nerve signal by minimizing the expected value of the squared difference between the estimate of the true signal (filtered signal) and the true, noiseless signal (Papoulis, 1984; Shanmugan and Breipohl, 1988). The contaminating noise is assumed to be additive and uncorrelated with the true signal. The result of Wiener filtering applied to the recording $x(t)$ is the estimate $\hat{s}$ of the true signal s, such that the expected value $E\{(s-\hat{s})^2\}$ is minimized. Matched filters are filters that maximize the S/N ratio of the filtered signal contaminated by additive noise (Papoulis, 1984), but do not estimate the true signal. In this work, finite impulse response (FIR) Wiener filters and infinite impulse response (IIR) realizations of the Matched filters were calculated using artificially generated nerve signals.

The filters were applied to electroneurograms recorded from the cat spinal nerve roots, whereby the recorded nerve activity originated from cutaneous, bladder, or rectal mechanoreceptors (of these, the cutaneous fibers transmit action potentials at the fastest conduction velocity, and the rectal afferent fibers at the slowest conduction velocity). For each recording a Wiener and a Matched filter that achieved the best S/N ratio improvement was calculated. The same recordings were also filtered with several band-pass (BP) filters that differed in cut-off frequencies, since the calculated optimal filters had a band-pass character. The improvements in the S/N ratios and the improvements in the modality selectivity (increased selectivity for cutaneous, bladder, or rectal receptor activation when appropriate filters designed for the same receptor type were used) were then assessed, and the results of all three filtering methods were compared.

2. Methods

2.1. Data acquisition

The electroneurograms were recorded from the cat S1 spinal nerve roots during acute experiments (Jezernik et al., 2001a). Data from four experiments (including nerve signals arising from bladder distensions, reflex bladder contractions, rectal distensions, and mechanical cutaneous stimulation) were used for filter design and analysis. All animal care and experimental procedures were according to NIH guidelines, and were reviewed and approved by the Institutional Animal Care and Use Committee of Case Western Reserve University. Intact male cats were anesthetized with ketamine HCl (Ketaset, 15–25 mg/kg, IM), a venous catheter was inserted in the cephalic vein, and anesthesia was maintained with α-chloralose (Sigma, 60 mg/kg, IV, supplemented at 15 mg/kg). Animals were intubated and respired, body temperature was maintained, and heart rate was continuously monitored. A transurethral catheter was inserted into the bladder, the urethra was ligated, and a balloon-tipped catheter was placed into the rectum. A laminectomy (L6–S3) was conducted and the extradural sacral roots were identified anatomically and by electrical stimulation. A silicone rubber cuff electrode containing two platinum ring contacts (25 μm thick platinum foil, 1.5 mm width) was placed unilaterally around the S1 extradural root. The cuffs were 10–15 mm in length for cuffs with two contacts inside the cuff and 6 mm long for cuffs with one contact inside and one contact outside the cuff, and had inner diameters of 1.0–1.8 mm. Electroneurograms were recorded during the excitation of bladder wall mechanoreceptors (spontaneous reflex bladder contractions, rapid injections of saline into the bladder), rectal mechanoreceptors (inflating the rectal balloon), and cutaneous receptors (manual stroking of the S1 dermatome). Nerve signals were preamplified (200–500 ×), filtered (100–3000 Hz), further amplified (1000–2000 ×), rectified, and time-averaged (time constant 200 ms). The rectified and time-averaged ENG will be denoted by $\langle|\mathrm{ENG}|\rangle$. The nerve signal preamplifiers were custom-made and had a constant gain over the frequency range of interest (-3 dB lower cut-off frequency was 150 Hz, -3 dB higher cut-off frequency was greater than 18 kHz). The preamplifier intrinsic root-mean-square noise level was 0.07 and 0.065 μV for the two preamplifiers respectively (for the frequency range of 100 Hz–3 kHz). The recorded signals were

digitized and stored on VCR tape. The raw ENG recordings were sampled off-line with a sampling frequency of 8 kHz, and the $\langle|\mathrm{ENG}|\rangle$ was sampled at 10 Hz. In the recordings made in cat 5 the nerve signals were also contaminated by power line noise that was removed digitally using narrow band-stop filters.

2.2. Filter design

2.2.1. B1. Wiener filter design

The digital FIR Wiener filter coefficients can be calculated using the discrete Wiener-Hopf equation (Papoulis, 1984; Shanmugan and Breipohl, 1988). The calculation requires the knowledge of the autocorrelation function r_{xx} of the measurement, $x(t)$, (where $x(t)=s(t)+n(t)$; $n(t)=$ noise), and the knowledge of the autocorrelation function r_{ss} of the true signal, $s(t)$. The filter coefficients, h, are given by Eq. (1):

$$R_{xx}=\begin{bmatrix} r_{xx}(0) & r_{xx}(1) & \dots & r_{xx}(N-1) \\ r_{xx}(1) & r_{xx}(0) & \dots & r_{xx}(N-2) \\ \vdots & \vdots & \ddots & \vdots \\ r_{xx}(N-1) & r_{xx}(N-2) & \dots & r_{xx}(0) \end{bmatrix}$$

$$R_{ss}=[r_{ss}(0)\ r_{ss}(1)\cdots r_{ss}(N-1)]^T \qquad (1)$$

$$h=R_{xx}^{-1}\ R_{ss}$$

The R_{xx} can be obtained from the recorded electroneurogram by a straightforward calculation, but it is usually difficult to estimate R_{ss} since the true signal $s(t)$ is not known. To resolve the latter problem, an artificial, noiseless nerve cuff signal $s(t)$ was generated by summation of randomly delayed single compound action potentials (CAPs). A prototype CAP was recorded in the pelvic nerve following a threshold stimulation of the S3 sacral root (averaged 20 times using triggering) (Jezernik and Sinkjaer, 1999). Sixty thousand time delayed prototype CAPs, each having a duration of 1 ms, were then summed in a 100 ms time window to yield the artificial nerve cuff signal (the time delays had uniform probability density function). Fig. 1 illustrates how the artificial nerve cuff signal was generated. The signal obtained by summation of 60 000 CAPs was sampled at 8 kHz (without the left and right boundaries) and used to calculate the generic autocorrelation function r_{ss}. This generic autocorrelation function was then modified (stretched in time) to match the characteristics of signals arising from cutaneous, bladder, and rectal mechanoreceptors, and to match the geometry of the recording electrode. The initial estimate of the optimal stretching factor was first calculated (using a selected real nerve signal) by least square fitting of the weighted real nerve signal autocorrelation function and the stretched generic autocorrelation function (Fig. 2). Different Wiener filters were then calculated using the initial estimate of the stretching factor and

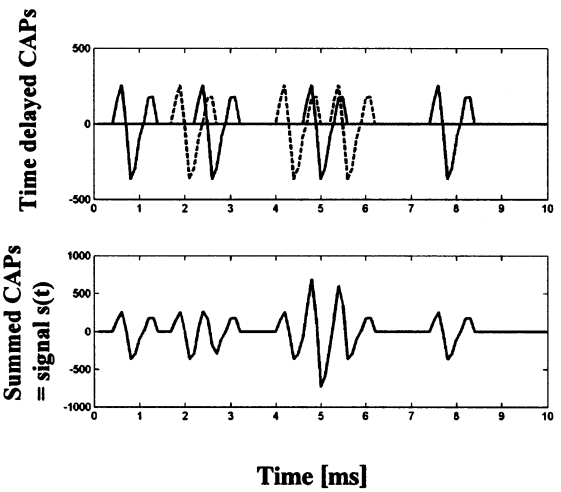

Fig. 1. Generation of the artificial, noiseless nerve cuff signal s(t). Prototype CAPs are delayed with random time-delays (top panel), and afterwards summed to obtain the signal s(t) (bottom panel). In this figure, only seven CAPs are summed in a 10 ms long time window, whereas in the subsequent calculations 60000 CAPs were summed in a 100 ms time window.

using stretching factors that deviated from the initial estimate of the stretching factor (integer multiples of steps ± 0.1 were used in forming the deviations). From these different stretching factors, the optimal stretching factor (the stretching factor that resulted in a filter that achieved maximal S/N ratio improvement) was then chosen to be used in the subsequent filtering and analysis (filters with the optimal stretching factor were therefore also called 'the best filters').

Ten thousand samples of the nerve recordings (1.25 s) were used to calculate the autocorrelation functions r_{xx}. The length of the filter, N, (range = 16–34) was chosen so that the autocorrelation function approached zero after N samples, and a sampling interval of 0.125 ms was used in all calculations ($f_s=8$ kHz).

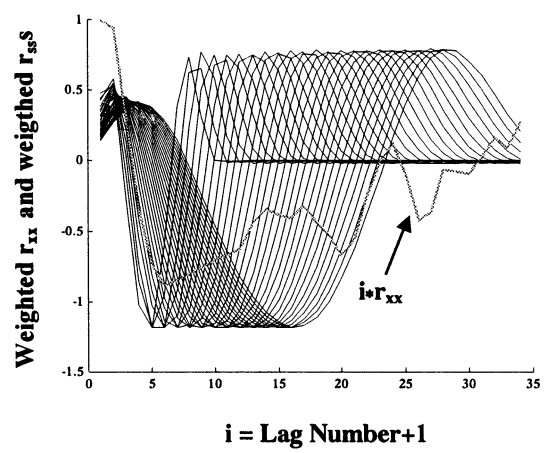

Fig. 2. Weighted least-square fitting of the r_{xx} with the stretched r_{ss}s to calculate the initial stretching factor estimate for the generic r_{ss}.

2.2.2. B2. Matched filter design

A Matched filter is an optimal filter that maximizes the S/N ratio of the filtered signal at time t_o. The calculation of its frequency response requires the knowledge of the power spectral density (psd) of the noise $N(\omega)$ and the true signal $S(\omega)$ (2) (Papoulis, 1984):

$$H(\omega) = k \frac{S^*(\omega)}{N(\omega)} e^{-j\omega t_0} \quad (2)$$

The psd of the noise was estimated from the signal recorded in the quiescent period before mechanical stimulation using the averaged spectrogram method, and the psd of the true signal was estimated/calculated by Discrete Fourier Transform of the stretched artificial nerve signal autocorrelation function described in the section on the Wiener filter design. This enabled calculation of the frequency response of the matched filters that were again calculated using different stretching factors to determine the filter that yielded maximal S/N ratio improvement (best Matched filter). The filters with the calculated frequency responses were realized by ARMA filters via the Yule–Walker iteration method that fitted only the amplitude of the frequency responses (and not the phase). These ARMA filter realizations of the calculated Matched filters were then applied to different recordings.

2.2.3. B3. Band-pass filter design

The band-pass filters were chosen as 4th order Butterworth filters with different lower and upper cut-off frequencies. For the nerve signals recorded during the cutaneous receptor activation, filters with the following frequency bands were calculated: 300–2000, 300–1750, 300–1500, 300–1250, 300–1000, 500–1000, 750–1000, 500–800, 500–1250, 750–1250 Hz. The frequency bands for the nerve signals recorded during the bladder receptor activation were 200–1500, 200–1250, 200–1000, 200–750, 200–600, 200–500, 300–600, 400–600, 450–550 Hz, and the frequency bands for the nerve signals recorded during the rectal receptor activation were 100–1000, 100–800, 100–600, 100–400, 200–600, 200–500, 200–1000, 200–1200 Hz. These cut-off frequencies were selected to enhance the frequency bands that were shown to contain information from the different receptor types according to the estimated power spectra of the signals recorded during receptor activation (Fig. 5). Band-pass filters, having the same cut-off frequencies as the -3 dB bandwidth of the corresponding best Wiener and Matched filter were also tested.

From all the above filters, the filter that yielded maximal S/N ratio improvement (best band-pass filter) was chosen for each animal and each receptor type and then applied to relevant recordings.

2.3. S/N ratio calculation

The S/N ratio is defined as the variance of the true signal, $s(t)$, divided by the variance of the noise, $n(t)$. Since the rectified and time-averaged nerve signal is proportional to the square root of the variance (Jezernik and Sinkjaer, 1999), the S/N ratio can be calculated from the amplitudes of the rectified and time-averaged signals as Eq. (3), where C was assumed to equal 1 in our calculations:

$$S/N = \frac{Var(s)}{Var(n)} = C \left[\frac{Ampl(\langle |s| \rangle)}{Ampl(\langle |n| \rangle)} \right]^2 \quad (3)$$

The improvement in the S/N ratio achieved after filtering can thus be assessed as:

$$\frac{S/N_{\text{filtered}}}{S/N_{\text{unfiltered}}} = \left(\frac{Ampl(\langle |s_{filtered}| \rangle)}{Ampl(\langle |s_{unfiltered}| \rangle)} \right)^2 \quad (4)$$

The ratio Eq. (4) was averaged over the part of the recording that contained the true signal (increase in the nerve activity due to receptor activation) after the noise levels of the filtered and unfiltered signals were adjusted to the same level.

2.4. Modality selectivity index

A modality selectivity index (MSI) was defined for recordings containing signals from two different sensory modalities, M_1 and M_2, to quantify modality selectivity of the nerve recordings. The MSI was defined as the quotient of the ratio of the amplitude of the two $\langle |\text{ENG}| \rangle$ signals (after the amplitude of the noise was subtracted) originating from different sensory modalities calculated after filtering, and of the ratio of the same two signals calculated before the filtering Eq. (5):

$$MSI = \frac{M_{1filtered}/M_{2filtered}}{M_{1unfiltered}/M_{2unfiltered}} \quad (5)$$

If filtering caused no change in the ratio of the two modalities, the MSI would equal one, in the case of decreased selectivity the MSI would be less than one (but greater than or equal to zero), and in the case of improved selectivity the MSI would be greater than one.

2.5. Statistical tests

The non-parametric Wilcoxon 2-sample Test and the Kruskal–Wallis Rank Sum Test were used to compare the performances of different filtering methods as the data were not normally distributed. The data were tested for differences in the S/N ratio improvements, and for differences in the MSI.

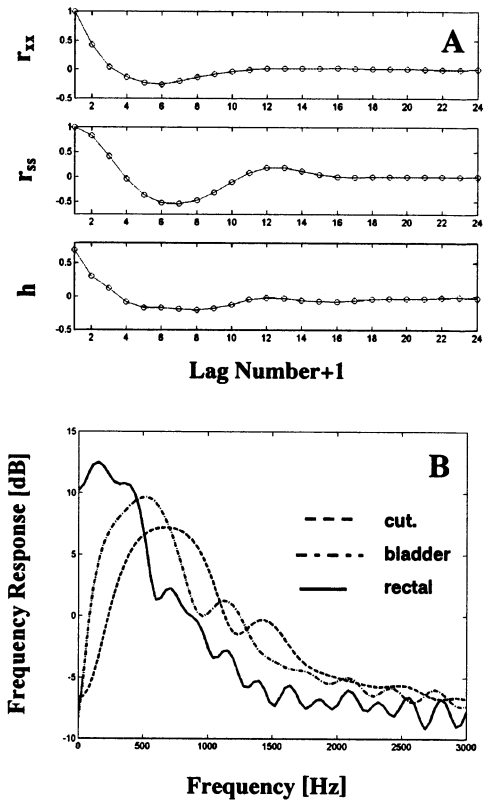

Fig. 3. A: Normalized autocorrelation function of the actual nerve cuff signal r_{xx} recorded during the activation of bladder receptors (first trace), normalized autocorrelation function of the stretched artificial nerve cuff signal r_{ss} (second trace), and the Wiener filter coefficients h calculated by Eq. (1) (third trace). The filter length was 24. B: Frequency responses of Wiener filters designed for cutaneous receptors (dashed line), for bladder mechanoreceptors (dashed-dotted line), and for rectal mechanoreceptors (solid line).

3. Results

3.1. A. Filter design

Examples of the normalized autocorrelation functions r_{xx} and r_{ss} used to calculate a Wiener filter for bladder receptors are depicted in Fig. 3A together with the impulse response of the filter h obtained from Eq. (1). The selected length N of this filter was 24, since the autocorrelation functions were close to zero after 24 samples. Because the measurement $x(t)$ contained noise, its autocorrelation function r_{xx} approached zero level faster that r_{ss}. The filtered signal was obtained by convolution of $x(t)$ with the impulse response of the Wiener filter h. Due to the bipolar cuff recording, the autocorrelation function first shows a negative sidelobe followed by a positive sidelobe. This shape results from the triphasic form of the recorded action potentials. The amplitudes of the frequency responses of the best Wiener filters designed for bladder mechanoreceptors, rectal mechanoreceptors, and cutaneous receptors (cat 6) are shown in Fig. 3B.

An example of the power spectral densities used to calculate a Matched filter are shown in Fig. 4A. $S(\omega)$ denotes the power spectral density of the constructed true signal, and $N(\omega)$ the estimated power spectral density of the noise. $|H(\omega)|$ is the resulting amplitude of the frequency response of the matched filter. The amplitudes of the frequency responses of the ARMA realizations of the Matched filters calculated for cat 6 are shown in Fig. 4B for comparison with those of the Wiener filters (Fig. 3B).

The Wiener and Matched filters behaved approximately as band-pass filters with center frequencies dependent on the type of receptor that was active and the stretching factors used in the filter design procedure. The stretching factors for filters that achieved maximal S/N ratio improvements are listed in Table 1. The peaks in the frequency responses of the Wiener and Matched filters for rectal and cutaneous receptors were shifted towards lower and higher frequencies respectively, as compared to the peak for the bladder mechanoreceptors. The explanation for this is that rectal (cutaneous) afferents have smaller (larger) axonal diameters and thus lower (higher) conduction velocities.

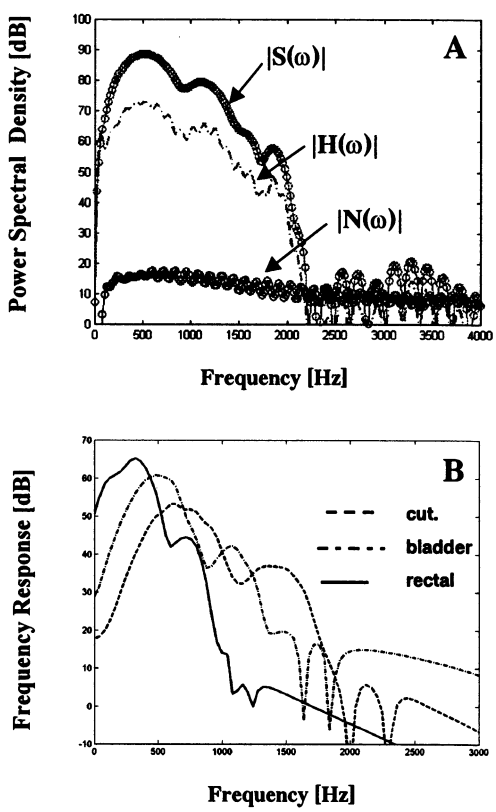

Fig. 4. Power spectral density amplitudes of the true signal S(ω) and of the noise N(ω) used to design the Matched filter together with their logarithmic difference (which equals the amplitude of the frequency response of the Matched filter, |H(ω)|). B: Frequency responses of Matched filters designed for cutaneous receptors (dashed line), for bladder mechanoreceptors (dashed-dotted line), and for rectal mechanoreceptors (solid line).

Table 1
Stretching factors used in the calculation of the Wiener and Matched filters that yielded the maximal S/N ratio improvement for each recording

Rec.	Animal	Receptors	Optimal BP freq. band [Hz]	Initial LS stretch factor	Optimal Wiener Filter stretch factor	Optimal Matched Filter stretch factor
1	Cat 1	Bladder	300–600	1.7	2.8	2.1
2	Cat 1	Bladder	200–500	1.7	2.6	2.3
3	Cat 1	Bladder	200–500	1.7	2.7	2.7
4	Cat 2	Bladder	400–600	2.1	2.1	1.9
5	Cat 2	Bladder	200–500	2.1	3.1	2.7
6	Cat 2	Bladder	400–600	2.1	2.5	2.1
7	Cat 2	Bladder	400–600	2.1	3.1	2.3
8	Cat 2	Cutaneous	750–1250	1.6	1.4	1.2
9	Cat 5	Cutaneous	750–1250	1.6	1.4	1.1
10	Cat 5	Rectal	200–1200	1.6	1.6	1.5
11	Cat 6	Rectal	200–600	3.3	2.7	2.5
12	Cat 6	Rectal	200–500	3.3	3.5	3.3
13	Cat 6	Bladder	200–1000	2.2	1.8	1.5
14	Cat 6	Bladder	400–600	2.2	2.1	2.3
15	Cat 6	Cutaneous	500–1000	1.7	1.6	1.6
16	Cat 6	Cutaneous	500–800	1.7	1.7	1.6

With a faster (slower) propagating action potential, the frequency content of the recorded nerve signal will lie at higher (lower) frequencies. The attenuation of the frequency bands that did not belong to the true signal was 7–20 dB for the Wiener filters, and >20 dB for the Matched filters.

The estimated power spectral densities of the nerve signals recorded during the activation of cutaneous, bladder, and rectal mechanoreceptors are shown in Fig. 5. The quality of the estimated power spectral densities was limited by the low S/N ratios. It can be observed that Wiener and Matched filters designed for specific receptor types attenuated mainly the frequency bands of the recorded signal that did not belong to the spectrum of the nerve signal (compare Figs. 3B, 4B, and 5).

3.2. B. Influence of the Filtering on the S/N Ratio

An example of the unfiltered and filtered nerve signals during a reflex bladder contraction (cat 1, recording 1 in Table 1) that activated bladder mechanoreceptors is shown in Fig. 6A for all three filtering techniques. In this example, the improvements in S/N ratio during the nerve signal increase were 137, 211, and 203% for the Wiener, Matched, and band-pass filtering respectively. An example of the unfiltered and filtered nerve signals during a rectal distension (cat 5, recording 10) is shown in Fig. 6B. In this example the increases in the S/N ratio of the nerve signal during rectal mechanoreceptor activation were 31, 52, and 37% for the Wiener, Matched, and band-pass filtering respectively. The baseline noise levels of filtered (100–3000 Hz), rectified, and time–averaged initial nerve recording were about 0.12 and 0.15 μV, respectively, for the two panels shown. The baseline noise level varied from animal to animal and sometimes also within the same animal due to the different recording electrodes used and due to changes in the electrode-tissue impedance that occurred during the course of experiments from electrode or nerve handling.

The S/N ratios of unfiltered nerve cuff signals across four animals together with the maximal improvements in the S/N ratios as achieved by different filtering methods are shown in Table 2 together with the average improvements for each animal, each receptor type, and each filtering method. Note that larger improvements were obtained in cats 1 and 2 compared to cats 5 and 6, as the levels of background noise were higher in the latter two experiments. This difference caused smaller improvements in S/N ratios for rectal and cutaneous afferent activity relative to the improvements during bladder afferent activation, as the former were primarily recorded in cats 5 and 6. The average improvements in S/N ratios

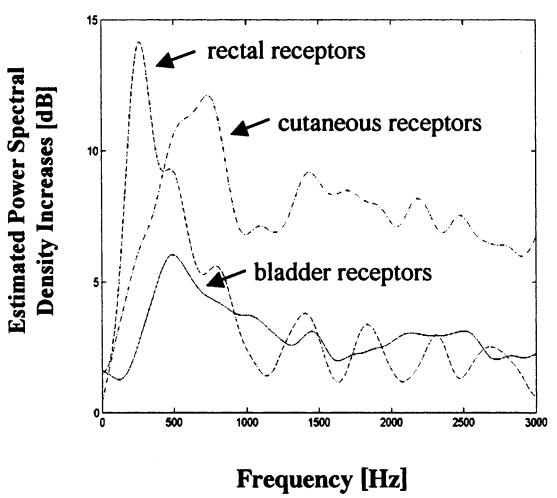

Fig. 5. The power spectral density increases of the nerve signals recorded during the activation of cutaneous, bladder, and rectal receptors.

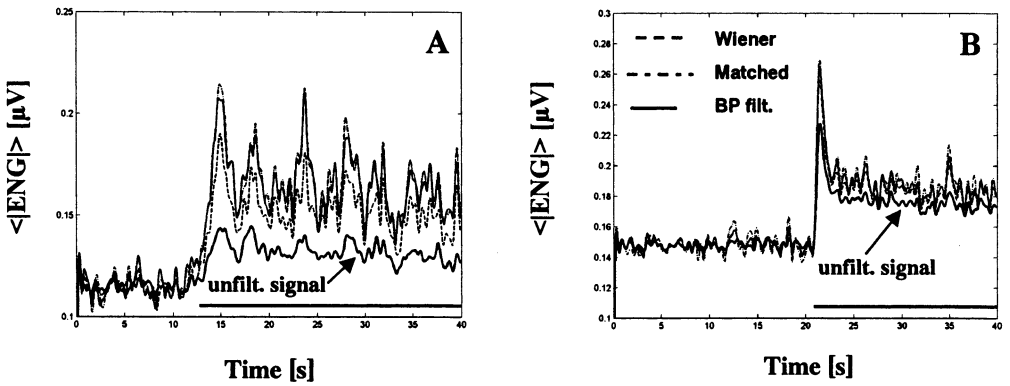

Fig. 6. A: Results of the Wiener, Mathced, and band-pass filtering during a reflex bladder contraction that activated bladder mechanoreceptors (indicated by a bar). The noise levels of the unfiltered and filtered signals were adjusted to the same level to allow assessment of an improvement in the S/N ratio. B: Wiener, Matched, and band-pass filtering of a nerve cuff signal increase originating from the activation of the rectal mechanoreceptors (mechanoreceptor activation is indicated by a bar). The initial steep increase in the recorded signal was probably also partly due to the activation of the cutaneous receptors, since inflating the rectal balloon in the distal part of the rectum also caused transient stretching of the perianal skin area.

achieved by the best Wiener, Matched, and band-pass filters were 54, 89, and 85%. The performance of the best filters did not differ significantly (Kruskal–Wallis χ^2 Test, $P > 0.0825$). The only statistically significant difference was found when comparing the performances of the Wiener and the Matched filters (Wilcoxon 2-Sample Test, $P < 0.0365$; Kruskal–Wallis Test, $P < 0.0348$).

The influence of the three filtering methods on the shape of the true signal was determined by examining the shape of the autocorrelation function of the filtered signal $x_{\text{filtered}}(t)$. The autocorrelation function of the Wiener filtered signal (Fig. 7, dashed line) most clearly resembles that of the estimated true signal (compare with the shape of r_{ss} in Fig. 3A), while the autocorrelation functions of the signals filtered with the Matched (Fig. 7, dash-dotted line) and band-pass (Fig. 7, thin solid line) filters did not replicate the shape of the true nerve signal's autocorrelation function. This means that both latter filters change the shape of the action potentials composing the true signal, whereas the Wiener filtering preserves the true action potential shape while minimizing the additive noise present in the recording.

3.3. C. Influence of the filtering on the modality selectivity

Wiener, Matched, and Band-pass filtering in most instances also improved the selectivity of the recordings for different sensory modalities. An example comparing selectivity between cutaneous and bladder afferents is shown in Fig. 8. The two panels illustrate the same recording (cat 2), which contained consecutive trials of cutaneous and bladder receptor activation, filtered using two different filters: in the first example by a Matched filter designed for cutaneous receptors (Fig. 8A), and in the second example by a Matched filter designed for bladder receptors (Fig. 8B). In the first case, the filtered nerve signal was larger than the unfiltered signal during the activation of cutaneous receptors, resulting in a 58% increase in the S/N ratio and a 1.29 times increase in the signal's amplitude (above the noise level). However, the filtered nerve signal's amplitude during the activation of bladder receptors increased only by 1.01 times the unfiltered signal. The same signal filtered with the Matched filter designed for bladder receptors was larger than the unfiltered signal during the activation of bladder receptors, resulting in a 92% increase in the S/N ratio and a 1.66 times increase in the signal's amplitude (above the noise level), whereas the average level of the filtered signal during the cutaneous receptor activation stayed the same. The modality selectivity indices calculated for the two filtered signals (Fig. 8A and B) were 1.27 and 1.66 respectively. The baseline noise levels were about 0.14 and 0.13 μV during the activation of cutaneous and bladder receptors, respectively. The two depicted recordings were concatenated off-line, i.e., the time between these two recordings was larger than shown, which also explains the change in the baseline noise level.

The summary data on changes in modality selectivity by filtering using each of the three methods are summarized in Table 3. The modality selectivity was increased in five of ten, seven of ten, and seven of ten combinations of two different sensory modalities for the Wiener, Matched, and band-pass filters respectively. All three filtering methods resulted in higher average MSI, but the differences between them were not statistically significant (Kruskal–Wallis Test, $P > 0.5724$).

The reason for all observed cases of decreased modality selectivity was that the S/N ratio increase of

Table 2
Signal to noise (S/N) ratios of unfiltered electroneurograms from four cats recorded during activation of different receptors, and the improvements in the S/N ratios achieved by different best filters[a]

Rec.	Animal	Receptor type	$10*\log(S/N)_{unfilt.}$ [dB]	Improvement in S/N ratio [%] — Wiener f.	Improvement in S/N ratio [%] — Matched f.	Improvement in S/N ratio [%] — BP filter
1	Cat 1	Bladder	−4.87	137.5	211.7	203.8
2	Cat 1	Bladder	−2.52	135	232.6	230.6
3	Cat 1	Bladder	−6.72	82.8	125.6	118.2
4	Cat 2	Bladder	−9.57	54.1	83.4	80.9
5	Cat 2	Bladder	−9.27	56.9	86.9	87.6
6	Cat 2	Bladder	−6.77	81.9	122	123.8
7	Cat 2	Bladder	−6.67	58	92.2	109.3
8	Cat 2	Cutaneous	−7.02	28.2	58.1	56.4
9	Cat 5	Cutaneous	−5.72	32.4	65.8	59.1
10	Cat 5	Rectal	−6.62	31	52	37.7
11	Cat 6	Rectal	−6.82	35.9	64.9	47.4
12	Cat 6	Rectal	−3.42	30.2	55.3	44.8
13	Cat 6	Bladder	−8.32	30.8	47.9	37.7
14	Cat 6	Bladder	−5.52	46	78.5	80.2
15	Cat 6	Cutaneous	−1.52	16.2	30.4	28.8
16	Cat 6	Cutaneous	−3.82	10.5	20.1	21.1
	Cat 1			118.4 ± 30.8	189.9 ± 56.7	184.2 ± 58.7
	Cat 2			55.8 ± 19.0	88.5 ± 22.8	91.6 ± 26.0
	Cat 5			31.7 ± 0.9	58.9 ± 9.7	48.4 ± 15.1
	Cat 6			28.2 ± 12.9	49.5 ± 21.6	43.3 ± 20.5
		Cutaneous		21.8 ± 10.2	43.6 ± 21.8	41.3 ± 19.2
		Bladder		75.8 ± 37.8	120.0 ± 62.5	119.1 ± 61.5
		Rectal		32.3 ± 3.0	57.4 ± 6.7	43.3 ± 5.0
Grand average				54.2 ± 37.9	89.2 ± 59.2	85.4 ± 60.4

[a] Shown are also the average improvements in S/N ratio (mean ± s.d.) for each animal and each receptor type

the signal recorded during sensory modality 2 was greater than the S/N ratio increase of the same signal recorded during sensory modality 1, when filtered with a filter designed for modality 1. Still, all three methods with appropriately designed filters could in most cases enhance the signal arising from specific receptor class and thus enhance the modality selectivity of the recording.

4. Discussion

The results of this study demonstrate that the S/N ratio and modality selectivity of neurographic recordings can be increased using optimal filtering. Most electroneurographic recordings suffer from low S/N ratios, and the increased S/N ratio will enable better signal detection (Goodall and Horch, 1992). Further, improved modality selectivity is important where there is a need to record selectively from subpopulations of nerve fibers present in a nerve trunk. For example, recording selectively bladder afferent information from the spinal sacral roots (Jezernik et al., 2001a,b), which also contain efferent and afferent fibers from rectum, skin and other viscera. The improvements in the modality selectivity were possible because the frequency spectra of the nerve signals differed during the activation of cutaneous, bladder, and rectal receptors.

The innovative development in the realization of the optimal filters was the generation of the artificial, noiseless nerve signal. This was accomplished by summation of CAPs recorded by a nerve cuff electrode following electrical stimulation of the proximal part of the nerve. The calculation of the Wiener filter coefficients, h, required the knowledge of the autocorrelation function of the artificial nerve cuff signal, r_{ss}. This r_{ss} was also used in the calculation of the Matched filters to estimate the power spectral density of the true signal $S(\omega)$.

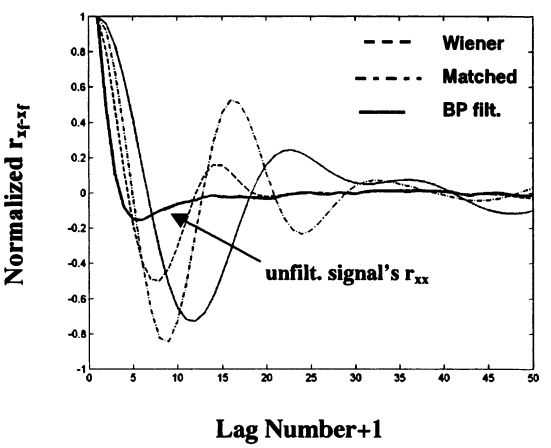

Fig. 7. The effect of different filtering techniques on the shape of the autocorrelation function of the filtered signal.

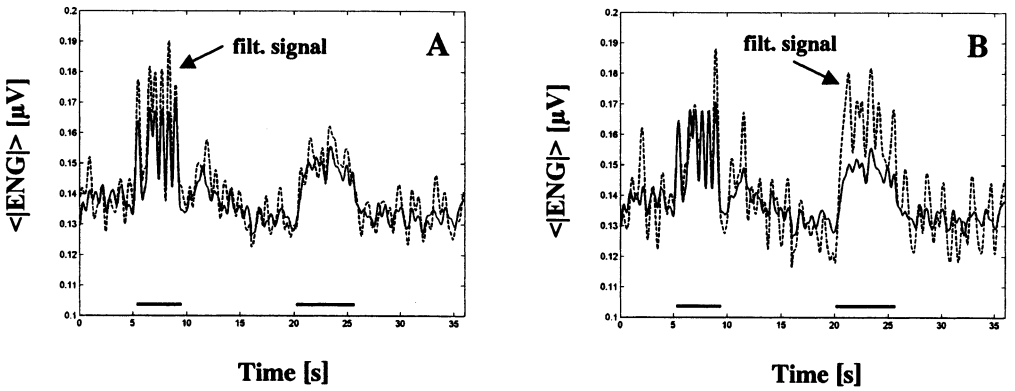

Fig. 8. Nerve cuff recording that contained activation of the cutaneous mechanoreceptors followed by an activation of bladder receptors (indicated by bars) was filtered with a Matched filter designed for cutaneous receptors (A), and with a Matched filter designed for bladder receptors (B). In (A), the filtered signal (dashed line) increased during cutaneous receptor stimulation, and also increased (but to a lesser extent) during the activation of bladder receptors. In (B), the filtered signal (dashed line) increased during bladder receptor stimulation, but stayed at the same average level during the activation of cutaneous receptors.

To achieve optimal matching of the filter characteristics and the recorded signal, only the nerve fibers targeted for recording should be active when recording the CAP, and the same electrode should be used to record the CAP as is used in the following recording experiments. Neither of these conditions was met in the present study and stretching of the autocorrelation function was used to achieve appropriate matching. With better matching during the CAP recording it is likely that even better results can be obtained. When using the CAP to estimate the single action potential shape, the dispersion of different action potentials (APs) travelling with different conduction velocities should be kept low. Thus, the distance between the stimulating and the recording electrodes should not be too large. Better results can likely also be achieved by employing methods to record single action potentials, rather than compound action potentials, and then using this action potential shape in the filter design procedure. In this case, matching of the geometries of the electrode(s) used to record the CAP or AP and the electrode(s) used in subsequent nerve recording will be required as well. Single fiber action potentials can also be estimated by using triggered signal averaging of nerve cuff recordings as described in Hoffer et al. (1981). This method would allow the use of the same nerve cuff electrode for both purposes (single AP shape estimation and subsequent nerve cuff recording).

Another question that needs to be addressed is whether the optimal filter parameters remain the same in the presence of EMG contamination of the nerve signal. The spectrum of an EMG signal has, in general, lower frequency content than the spectrum of an ENG signal, but in case of low nerve fiber conduction velocity, the two spectra might overlap. To get an optimal estimate of the nerve signal only, an additional attenuation (low-pass filtering) might be needed to suppress the EMG. EMG contamination was absent in our acute experiments, as confirmed by test recordings where the baseline of the signal remained constant during activation of different receptors (with nerves transected proximally and distally to the recording electrodes). This also means that, even if reflexly evoked, no EMG was picked up by the cuff electrodes.

The frequency responses of the Wiener and Matched filters were similar to frequency responses of band-pass filters. Therefore, a properly chosen band-pass filter can be used instead of an optimal filter to achieve approximately maximal S/N ratio improvements. This was confirmed by the Kruskal-Wallis Test that showed no significant statistical difference in the performances of best Matched filters and best band-pass filters. The performance of the realized Wiener and Matched filters was most likely suboptimal, which was due to inaccurate true signal (artificially generated nerve cuff signal) used in the filter design.

However, from the three filtering methods presented, only a Wiener filter is able to estimate optimally (in a least-mean-squares sense) the true signal's shape, and therefore the true r_{ss}. On the other hand, the increases in the S/N ratio achieved by the Wiener filtering were smaller than the increases achieved by Matched filtering or band-pass filtering. This can be explained as the Wiener filter reduces noise only by forming a better estimate of the true signal, and therefore does not optimize the actual S/N ratio.

The described filter design procedure can also be used for other electroneurographic recordings, which widens its applicability. Importantly, digital filtering can be easily implemented in real-time with the use of digital signal processing hardware.

Table 3
Modality Selectivity Indices calculated for different combinations of two sensory modalities filtered with appropriate filters. The used filters were the filters that yielded maximal S/N ratio improvements for the modality M1

Animal	M_1	M_2	MSI — Wiener f.	MSI — Matched f.	MSI — BP f.	BP freq. band [Hz]
Cat 2	Cutaneous	Bladder	0.984	1.272	1.284	750–1250
	Bladder	Cutaneous	1.543	1.664	1.904	400–600
Cat 5	Cutaneous	Rectal	1.035	1.202	1.126	750–1250
	Rectal	Cutaneous	0.975	1.05	0.96	200–1200
Cat 6	Cutaneous	Bladder	0.838	0.803	0.837	500–1000
	Bladder	Cutaneous	1.382	1.877	1.797	400–600
	Cutaneous	Rectal	0.943	0.946	1.109	500–1000
	Rectal	Cutaneous	1.484	1.953	1.877	200–600
	Bladder	Rectal	1.085	1.094	1.141	400–600
	Rectal	Bladder	0.937	0.92	0.937	200–600
Average MSI:			1.12 ± 0.25	1.27 ± 0.41	1.29 ± 0.40	

5. Conclusions

A method to design the Wiener and Matched filters for neurographic recordings was developed and applied to nerve cuff signals recorded from the cat S1 sacral root during activation of cutaneous, bladder and rectal receptors. Appropriately designed optimal filters improved the S/N ratios of the nerve signals by 10–137% (range of the Wiener filtering improvements) and by 20–232% (range of the Matched filtering improvements). The frequency responses of optimal Wiener and Matched filters were found to have a band-pass character. Therefore, band-pass filters having different cut–off frequencies were also applied to the same set of the sacral root recordings and their performance in improving the S/N ratios (range 21–230%) was compared to that of the optimal filters. All three filtering techniques also increased the modality selectivity of most recordings due to differences in the frequency spectra of the nerve signals recorded during the activation of cutaneous, bladder and rectal receptors. These differences arise only in case where different types of nerve fibers transmit action potentials at significantly different conduction velocities.

There was no statistically significant difference between the performance of the selected best Matched filters and best band-pass filters. Improving the S/N ratio and modality selectivity of neurographic recordings is an important development to increase the utility of neural signals for understanding neural function and for use as feedback or control signals in neural prosthetic devices.

Acknowledgements

The authors would like to thank Dr Mesut Sahin for using his preamplifiers during the cat experiments. This study was supported by The Danish National Research Foundation, The Danish National Research Council, and the Johnson & Johnson Focused Giving Program.

References

Goodall EV, Horch KW. Separation of action potentials in multiunit intrafascicular recordings. IEEE Trans Biomed Eng 1992;39:289–95.

Hoffer JA, Loeb GE, Pratt CA. Single unit conduction velocities from averaged nerve cuff electrode records in freely moving cats. J Neurosci Methods 1981;4:211–25.

Hoffer JA. Techniques to study spinal-cord, peripheral nerve, and muscle activity in freely moving animals. Neurometh: Neurophysiol Tech Appl Neural Syst 1990;15:65–145.

Jezernik S, Sinkjaer T. On statistical properties of whole nerve cuff recordings. IEEE Trans Biomed Eng 1999;46:1240–5.

Jezernik S, Grill WM, Sinkjaer T. Detection and inhibition of hyperreflexive-like bladder contractions in the cat by sacral nerve root recording and electrical stimulation. Neurourol Urodyn 2001a (in press).

Jezernik S, Grill WM, Sinkjaer T. Neural Network Classification of Nerve Activity Recorded in a Mixed Nerve. Neurol Res 2001b (In press).

Loeb GE, Peck RA. Cuff electrodes for chronic stimulation and recording of peripheral nerve activity. J Neurosci Methods 1996;64:95–103.

Nikolic ZM, Popovic DB, Stein RB, Kenwell Z. Instrumentation for ENG and EMG recordings in FES systems. IEEE Trans Biomed Eng 1994;41:703–6.

Papoulis A. Probability, Random Variables, and Stochastic Processes', 2nd edn. McGraw-Hill, 1984:298–300.

Popovic DB, Stein RB, Jovanovic KL, Dai R, Kostov A, Armstrong WW. Sensory nerve recording for closed-loop control to restore motor functions. IEEE Trans Biomed Eng 1993;40:1024–31.

Shanmugan KS, Breipohl AM. Random signals: Detection, Estimation and Data Analysis. John Wiley & Sons, 1988:377–474.

Sinkjaer T, Haugland M, Struijk JJ, Riso R. Long-term cuff electrode recordings from peripheral nerves in animals and humans. In: Windhorst U, Johansson H, editors. Modern Techniques in Neuroscience. Springer–Verlag, 1999.

Stein RB, Pearson KG. Predicted Amplitude and form of action potentials recorded from unmyelinated nerve fibers. J theor Bio 1971;32:539–58.

Struijk JJ. The extracellular potential of a myelinated nerve fiber in an unbounded medium and in nerve cuff models. Biophys J 1997;72:2457–69.

Upshaw B, Sinkjaer T. Digital signal processing algorithms for the detection of afferent nerve activity recorded from cuff electrodes. IEEE Trans Reh Eng 1998;6:172–81.